AEM system target resolvability analysis using a Monte Carlo inversion algorithm

Ross C Brodie
Geoscience Australia
GPO Box 378
Canberra, ACT 2601
ross.c.brodie@ga.gov.au

Murray Richardson
Geoscience Australia
GPO Box 378
Canberra, ACT 2601
murray.richardson@ga.gov.au

SUMMARY

A reversible-jump Markov chain Monte Carlo inversion is used to generate an ensemble of millions of models that fit the forward response of a geoelectric target. Statistical properties of the ensemble are then used to assess the resolving power of the AEM system.

Key words: Monte Carlo, AEM, inversion, resolvability.

INTRODUCTION

There are several factors that must be considered when choosing an airborne electromagnetic (AEM) system for a specific survey task. These factors always include cost, availability and logistics. However, the most important consideration is the ability of an AEM system to resolve the target(s) to be mapped.

To date Geoscience Australia has tackled this later consideration in terms of "detectability" rather than the "resolvability", which are two distinct concepts. We say that a target is detectable if the difference between the AEM response of the target and the background is sufficiently greater than the AEM system's noise levels. Resolvability not only requires that the target's data anomaly be detectable, but that we can also estimate, with sufficient confidence, via an inversion procedure, the cause of the anomaly.

Geoscience Australia is now addressing the resolvability question though a reversible jump Markov chain Monte Carlo (rj-McMC) inversion algorithm. A 1D forward model code generates synthetic data for each AEM system under consideration. This occurs for a suite of type-model scenarios that represent the expected range of situations to be mapped, and may include actual downhole conductivity logs. The data are then inverted using the rj-McMC inversion which, importantly, uses independently estimated AEM system noise levels.

The rj-McMC algorithm samples millions of models, possibly on independent parallel Markov Chains, that fit the data to within the AEM system's expected noise levels. Analysis of the ensemble of models yields a robust estimate of the uncertainty of resolving the model at any particular depth. It is a simple matter to then compare and contrast the results for each AEM system under consideration. We also show how the method can be used to provide depth of investigation estimates.

METHOD

We use a software program for 1D rj-McMC inversion of AEM data developed at Geoscience Australia. The methodology, previously described by Brodie and Sambridge (2012), was adapted from the 2D seismic tomography inversion work of Bodin and Sambridge (2009). Similar techniques in the geophysical literature include Malinverno (2002) and Minsley (2012). The software was also used in the inversion of an entire SkyTEM™ survey flown in Western Australia (Brodie and Reid, 2013, this volume).

The rationale of the rj-McMC inversion method is to generate a large ensemble of models that fit the data to within the assigned noise levels. The ensemble is generated using random perturbations of an initial model, and hence it is a Monte Carlo technique. However, the perturbations are not entirely random. Instead, they are generated using Markov chain sampling theory, which means that the ensemble is generated in such a fashion that the statistical distribution of the models in the output ensemble asymptotically converges to the true posterior probability distribution of the model parameters given the prior knowledge and the observed data. Then, by analysing the statistical properties of the output ensemble, insights into the uncertainty and non-uniqueness of the inversion results are realised.

The reversible jump (rj) terminology arises from the fact that it falls into the relatively new transdimensional class of McMC methods (Green, 1995), in which the number of dimensions in the problem is not fixed. This means that we do not presuppose the number of layers in our 1D conductivity model. The mechanics of the algorithm is briefly outlined here.

A feasible model domain, that is, a minimum and maximum: number of layers; depths of interfaces; and range of possible conductivity values; is defined. A Markov chain, or possibly multiple independent chains, is initialised with a random model taken from the feasible domain.

Then, in a sampling loop starting from the current model $\boldsymbol{m}$, a new model $\boldsymbol{m'}$ is proposed in one of four possible ways: (i) *VALUE-CHANGE* - a layer's conductivity is perturbed; (ii) *MOVE* - an interface is moved up or down; (iii) *BIRTH* - a layer is inserted; and, (iv) *DEATH* - a layer is deleted. The perturbations in each case are randomly selected from certain pre-set proposal probability distributions.

The next step is to decide if the proposed model is accepted or rejected. To do this, the prior probabilities of the current ($p(\boldsymbol{m})$) and proposed ($p(\boldsymbol{m'})$) models are computed from any prior information. Forward models are run and then the likelihood functions, which increase with decreasing noise normalized data misfit, of the current ($p(\boldsymbol{d}|\boldsymbol{m})$) and proposed ($p(\boldsymbol{d}|\boldsymbol{m'})$) models, given the data ($\boldsymbol{d}$), are computed. Then the probability of the forward jump ($q(\boldsymbol{m'}|\boldsymbol{m})$) from the current to proposed, and reverse jump ($q(\boldsymbol{m}|\boldsymbol{m'})$) given the proposal distributions, are computed.

The proposed model is then accepted and added to the end of the chain with probability

$$\alpha(\mathbf{m}' \mid \mathbf{m}) = \min\left[1, \frac{p(\mathbf{m}')}{p(\mathbf{m})} \times \frac{p(\mathbf{d} \mid \mathbf{m}')}{p(\mathbf{d} \mid \mathbf{m})} \times \frac{q(\mathbf{m} \mid \mathbf{m}')}{q(\mathbf{m}' \mid \mathbf{m})}\right],$$

otherwise it is rejected and a copy of the current model is added to the end of the chain. The process of accepting or rejecting models controls the sampling of the Markov chain. It ensures that the chain asymptotically converges to the true $p(\boldsymbol{m}|\boldsymbol{d})$, that is the posterior probability density of the model given the observed data.

Each chain generates N_s models, including the burn-in period N_b that gives time for an acceptable data misfit to be achieved. After the burn-in, new models are added into a discretized 2D posterior probability histogram. That is, for each discrete histogram depth-bin, the model conductivity is determined and the corresponding histogram conductivity-bin count is incremented. This progressively builds up an image representation of the desired $p(\boldsymbol{m}|\boldsymbol{d})$. Similarly, a 1D changepoint histogram is built up by incrementing all depth-bins of the 1D histogram in which a layer interface falls.

For the value-change move propositions, the sampling algorithm favours accepting models with high likelihoods (low data misfits) and high prior likelihoods. For the birth and death propositions the acceptance probability is also a balance between the proposal probability, which encourages conductivity changes, and the difference in data misfit, which penalizes conductivity changes if they degrade data fit. Also, given similar data fits, a proposed model has more chance of being accepted if $\boldsymbol{m'}$ has fewer layers than $\boldsymbol{m}$, giving the algorithm a form of natural parsimony.

At the conclusion of the sampling the 2D probability density histograms and the changepoint histograms are merged. Several statistics are then extracted from the histograms including the mean, mode, median, 10th, 50th, and 90th percentiles log-conductivity values in each depth bin. Also the single most probable (best) model from all chains is saved. It is the distance or spread between the 10th and 90th percentile models that we use to make assessments about resolvability; the narrower the spread the better the resolution.

EXAMPLES

To carry out the resolvability analysis for a particular 1D geoelectric target and AEM system a 1D forward model is run for the geoelectric target for that AEM system in its nominal configuration. Then we invert the dataset using the rj-McMC algorithm. Here we will show three examples that have been run for the SkyTEM508™ and TEMPEST™ systems. In all cases we assigned a feasible model domain with conductivity limits from 0.001 S/m to 10 S/m, with up to 10 layers possible and a maximum interface depth of 200 m.

The prior probabilities distributions for the number of layers and interface depths are set to uniform, and log-uniform on the conductivities (conductivity is parameterized in log). Uniform priors are used to ensure our results are only being influenced by the raw resolving power of the AEM system itself, and not by artificial model constraints.

To arrive at a robust estimate of resolvability, it is necessary to test a broad spectrum of models that satisfy the data. Testing only those models with the same number of layers as the target model would have the propensity to derive an unrealistically optimistic resolving ability. We achieve this by letting the rj-McMC algorithm vary the number of layers.

We do not add synthetic noise to the data because our noise model for the AEM system is taken into account during the inversion. As noted earlier, the likelihood function depends on a noise normalized data misfit. Consequently, all other things being equal, with increasing noise levels the sampling algorithm will automatically test a broader part of model space and hence the spread between the 10th and 90 percentile model will increase. Assigning realistic noise levels is therefore a crucial part of the procedure.

For the examples presented here we inverted the Z-component of the Low- and Super-High moments of the SkyTEM508™ data together (36 windows in total). A noise model of 3.6% multiplicative noise plus a high altitude data-derived additive noise floor was used for each window. For TEMPEST™ we inverted the X- and Z-component data together (30 windows in total). A noise model of 2.3% (X) and 3.8% (Z) plus a high altitude data-derived additive noise floor was used.

One million models were sampled on 16 independent Markov chains run in parallel for each model with a burn-in period of 100,000 samples before samples are incorporated into the output histograms. Each of the figures following contain the same style of plots, so they will be explained only once here. Panel (a) of each figure shows the convergence profile of each of the 16 Markov chains. It can be seen that they always converge to the acceptable data misfit (horizontal red line) well before the burn-in period (vertical red line). Note that the data misfits are not normalized by the number of data. Thus the number of data, 36 and 30 respectively for SkyTEM508™ and TEMPEST™, are the acceptable misfits.

In the first example the resolvability of a saline aquifer at around 60 to 80 m depth is tested. The true geoelectric model, derived from real downhole resistivity log data, is shown in Figures 1b and 2b. The grey shading on panel (b) depicts the posterior probability density distribution (i.e., the counts in the 2D output histogram). The red lines show the position of the 10th and 90th percentile of the conductivity values across each row (depth-bin) of the histogram.

It is clear from Figures 1b and 2b that both SkyTEM508™ and TEMPEST™ will both easily detect and broadly resolve the aquifer. However, the details of the double-peaked shape of the conductivity bulge will not be resolved, because it cannot be distinguished from a broader and less conductive bulge. Since the 10th and 90th percentile lines practically overlie the true model in the top 60 m we can confidently say that part of the profile is very well constrained by the data of both systems.

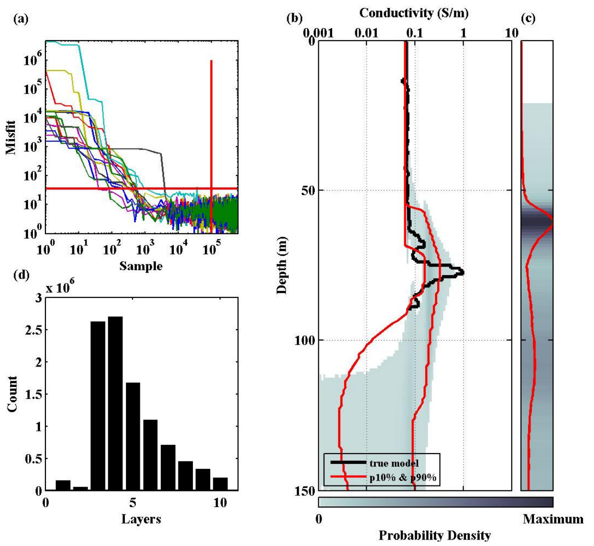

Figure 1. SkyTEM508™ results for the saline aquifer example showing the (a) misfits on each Markov chain, (b) the true model, probability density histogram and 10*th* and 90*th* percentile models, (c) changepoint histogram, and (d) histogram of the number of layers.

Figures 1c and 2c show the changepoint histograms. These histograms indicate the depth at which interfaces were most likely to occur in the models that were accepted into the Markov chains. The grey shading and the red line show the same information, just in a different manner. We can infer from these that the interface at the top of the saline aquifer around 60 m is resolved but that the bottom is not at all well resolved. Further, we can infer from the relative widths of the peaks in Figure 1c and 2c, that SkyTEM508™ would probably resolve the depth better than TEMPEST™.

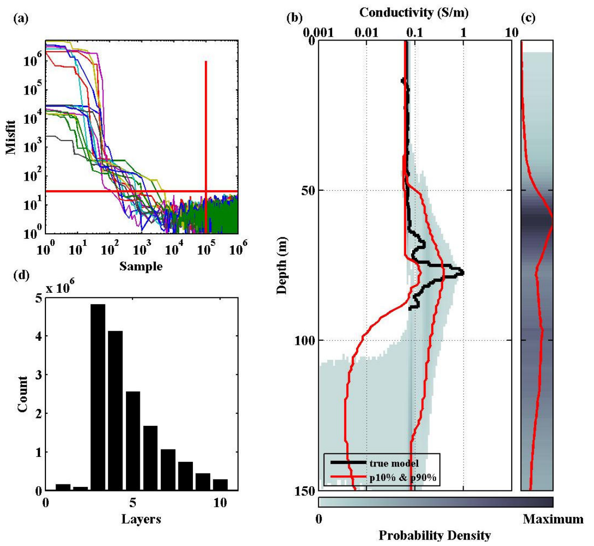

Figure 2. TEMPEST™ results for the saline aquifer example showing the (a) misfits on each Markov chain, (b) the true model, probability density histogram and 10*th* and 90*th* percentile models, (c) changepoint histogram, and (d) histogram of the number of layers.

Figures 1d and 2d indicate that a three layer model is the most probable. One or two layers will not typically be able to explain the data. However three layers is sufficient, which is consistent with our earlier observation that the double-peaked bulge will generally be resolved as a single broader but less conductive layer.

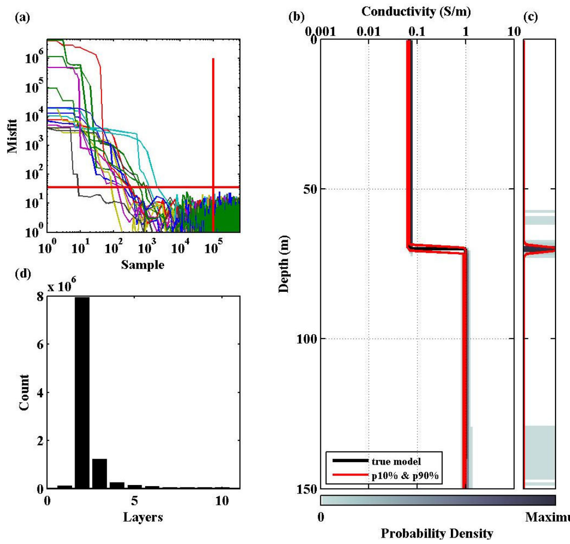

Figure 3. SkyTEM508™ results for the regional saline intrusion example showing the (a) misfits on each Markov chain, (b) the true model, probability density histogram and 10*th* and 90*th* percentile models, (c) changepoint histogram, and (d) histogram of the number of layers.

The second example, whose geoelectric model is shown in Figure 3b and 4b, mimics a regional salt water interface at 70 m depth and continuing to great depth. These plots show that the conductivity above and below the interface at 70 m would be very well resolved by both systems. The changepoint histograms also show that the depth of the salt water would also be well resolved.

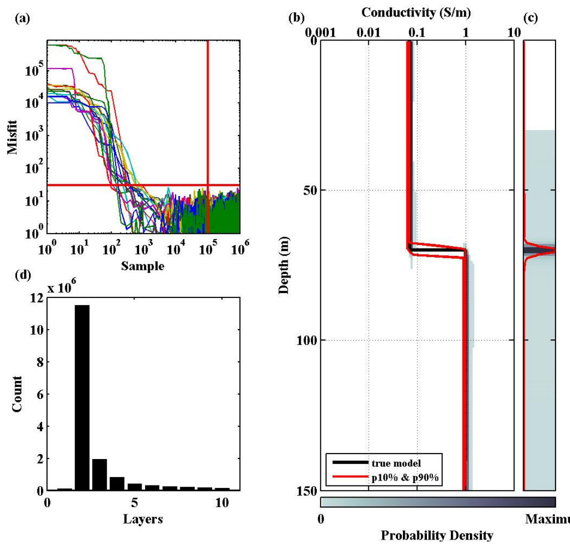

Figure 4. TEMPEST™ results for the regional saline intrusion example showing the (a) misfits on each Markov chain, (b) the true model, probability density histogram and 10*th* and 90*th* percentile models, (c) changepoint histogram, and (d) histogram of the number of layers.

The third example is a much more difficult task for AEM systems. The geoelectric model, shown in black in Figures 5b and 6c, is a thin (5 m) clay layer with a 0.100 S/m conductivity embedded in a 0.030 S/m host at 20 m depth.

The grey shading and the 10th and 90th percentiles on Figure 5b gives a hint of an elevated conductivity at 20 m depth for SkyTEM508™, but it is not evident for TEMPEST™ in Figure 6b. The clay layer is generally smeared as a much broader and less conductive layer than it really is. The changepoint histograms do not show any evidence of resolution of the interfaces for either system. Furthermore the histograms of the number of layers (Figure 5d and 6d) show, especially in the case of TEMPEST™, that two layers is sufficient to explain the data.

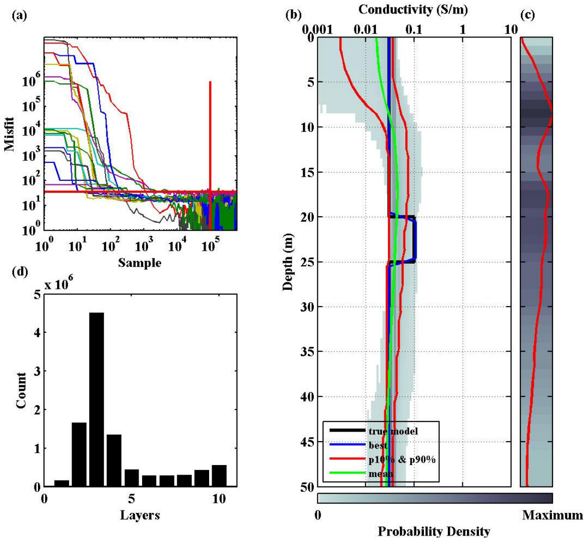

Figure 5. SkyTEM508™ results for the clay layer example showing the (a) misfits on each Markov chain, (b) the true model, probability density histogram and 10*th* and 90*th* percentile models, (c) changepoint histogram, and (d) histogram of the number of layers.

This is nice example of a geoelectric model that we would describe as detectible but not resolvable by these two systems. However, in this case we can be relatively confident that SkyTEM508™ would be the more suitable system.

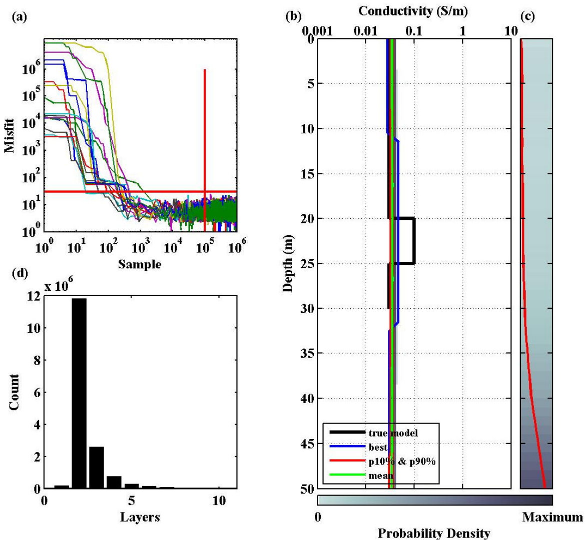

Figure 6. TEMPEST™ results for the clay layer example showing the (a) misfits on each Markov chain, (b) the true model, probability density histogram and 10*th* and 90*th* percentile models, (c) changepoint histogram, and (d) histogram of the number of layers.

For this example two additional traces have been plotted on panel (b), the mean model (green) and most probable or best model (blue). The mean model is more or less a smoothed version of the true model, and probably contains the same amount of conductance.

The best model for the SkyTEM508™ system is almost identical to the true model. However, and most importantly, this is in no way any indication of resolvability, rather it is just one of about 14 million models that happened to satisfy the data. Of course, since the anomaly is detectable above noise levels, at least with SkyTEM508™, this situation can be improved with conductivity constraints imposed during any suitable inversion procedure.

CONCLUSIONS

The rj-McMC inversion algorithm provides a powerful method for analysing the raw resolving power of an AEM system. The underlying inversion is quantitative, but interpretation of the results is still qualitative. The method robustly uses AEM system noise levels in the analysis. However, for the results to be worthwhile, the levels assigned to the noise need to be representative. The method makes a clear distinction between detectability and resolvability.

ACKNOWLEDGMENTS

The computational work was carried out on the National Computational Infrastructure (NCI, http://www.nci.org.au). The NCI is supported by the Australian Government through the Department of Innovation, Industry, Science and Research and by a number of major co-investing partner organisations including the Australian National University, CSIRO, the Australian Bureau of Meteorology and Geoscience Australia. This work is published with the permission of the CEO of Geoscience Australia.

REFERENCES

Bodin, T., and Sambridge, M., 2009, Seismic tomography with the reversible jump algorithm. Geophysical Journal International 178, 1411-36.

Brodie, R., and Reid, J., E., 2013, Monte Carlo Inversion of SkyTEM AEM data from Lake Thetis, Western Australia: 23rd International Geophysical Conference and Exhibition, Australian Society of Exploration Geophysicists, Extended Abstracts.

Brodie, R., and Sambridge, M., 2012, Transdimensional Monte Carlo Inversion of AEM Data: 22nd International Geophysical Conference and Exhibition, Australian Society of Exploration Geophysicists, Extended Abstracts.

Green, P.J., 1995, Reversible jump MCMC computation and Bayesian model selection. Biometrika 82, 711–32.

Malinverno, A., 2002, Parsimonious Bayesian Markov chain Monte Carlo inversion in a nonlinear geophysical problem. Geophysical Journal International 151, 675-88.

Minsley, B.J., 2011, A trans-dimensional Bayesian Markov chain Monte Carlo algorithm for model assessment using frequency-domain electromagnetic data. Geophysical Journal International 187, 252-72.